

**Boundary-structure determination of Ag/Si(111) interfaces by x-ray diffraction**

R. D. Aburano

*Materials Research Laboratory, University of Illinois, 104 South Goodwin Avenue, Urbana, Illinois 61801-2902  
and Department of Physics, University of Illinois, 1110 West Green Street, Urbana, Illinois 61801-3080*

Hawoong Hong

*Materials Research Laboratory, University of Illinois, 104 South Goodwin Avenue, Urbana, Illinois 61801-2902*

J. M. Roesler

*Materials Research Laboratory, University of Illinois, 104 South Goodwin Avenue, Urbana, Illinois 61801-2902  
and Department of Physics, University of Illinois, 1110 West Green Street, Urbana, Illinois 61801-3080*

K. Chung

*University of Illinois, 104 South Goodwin Avenue, Urbana, Illinois 61801-2902  
and Department of Materials Science and Engineering, University of Illinois, Urbana, Illinois 61801*

D.-S. Lin

*Department of Physics, National Chiao-Tung University, Hsinchu, Taiwan, Republic of China*

P. Zschack

*Metals and Ceramics Division, Oak Ridge Institute for Science and Education, Oak Ridge, Tennessee 37831*

H. Chen

*Materials Research Laboratory, University of Illinois, 104 South Goodwin Avenue, Urbana, Illinois 61801-2902  
and Department of Materials Science and Engineering, University of Illinois, Urbana, Illinois 61801*

T.-C. Chiang

*Materials Research Laboratory, University of Illinois, 104 South Goodwin Avenue, Urbana, Illinois 61801-2902  
and Department of Physics, University of Illinois, 1110 West Green Street, Urbana, Illinois 61801-3080*

(Received 6 March 1995)

Different Ag/Si(111) systems have been examined using synchrotron x-ray diffraction. Multi-atomic-layer deposition of Ag onto a Si(111)-(7×7) surface maintained at room temperature results in an unstrained, (111)-oriented film. The interface shows a Ag-modified (7×7) structure which when annealed above 200–250 °C transforms to a (1×1) structure. Although this is near the characteristic temperature for formation of the  $(\sqrt{3}\times\sqrt{3})R30^\circ$  surface reconstruction commonly observed for a monolayer of Ag adsorbed on Si(111), no evidence of this  $(\sqrt{3}\times\sqrt{3})R30^\circ$  reconstruction was found at the interface. A Ag monolayer  $(\sqrt{3}\times\sqrt{3})R30^\circ$  surface, further covered by multilayer Ag deposition at room temperature, also shows no indication of the  $(\sqrt{3}\times\sqrt{3})R30^\circ$  reconstruction at the interface. This indicates that the actual interface structure may or may not be related to the clean or adsorbed layer structures. The structure of the Ag-Si interface was further characterized by scans of the crystal truncation rods. Both the (7×7) interface prepared by room-temperature deposition and the annealed (1×1) interface show fairly sharp boundaries. The results suggest some intermixing occurs at the monolayer level for the annealed interface. The structure of the Ag film was also investigated.

**I. INTRODUCTION**

The investigation of interfaces is a fundamentally interesting and technologically promising field of study. Their properties depend to a significant degree on the atomic interface structure. This structure is itself dependent upon a number of factors.<sup>1</sup> These include those related to the materials themselves and those related to the interface formation process. The chemical reactivity, interdiffusion, lattice matching, bonding configuration, and substrate template are examples of the former, while

surface cleanliness, deposition rate, and substrate temperature are examples of the latter. The proper control of these parameters is the key to producing boundary structures, which have the desired macroscopic properties.

Results of this interfacial engineering have already shown promise. It is well documented that at least one physically important macroscopic observable is associated with the structure at the interface. For example, Tung,<sup>2</sup> Heslinga *et al.*,<sup>3</sup> Weitering *et al.*,<sup>4</sup> Schmitsdorf, Kampen, and Mönch,<sup>5</sup> and Mönch<sup>6</sup> have shown that the Shottky barrier height of metal-silicon interfaces depends

on the interfacial structure. This possibility for the atomic engineering of the boundary between two different materials may open the door to a wide range of potential applications.

It is interesting to compare properties about the boundary between materials to characteristics measured for low-coverage adsorbed structures. Any correlations would be beneficial since there are relatively few surface science methods that can probe an interface deeper than a few atomic layers. In our research, we employ x-ray crystallography, which determines a structure by measuring both the in-plane (parallel) and out-of-plane (perpendicular) momentum transfers. The considerable penetration depth of x rays in matter allows us to probe the buried interface and to investigate any possible correlations with clean and low-coverage adsorbate structures. In general, observed clean or monolayer (ML) adsorbate structures found at a buried interface would be a surprising result, since these structures are formed without the disturbance or interaction of future deposited layers. However, clean and adsorbate surface reconstructions have been found to persist at buried interfaces in certain systems.<sup>7-12</sup> Not surprisingly, these interfacial superstructures are modified from the clean or adsorbate structure to varying degrees resulting from the deposition and interaction with the deposited material. The wide range of behavior demonstrates the need to consider each system separately or at the very least, each family of systems.

In this work, we present results from our investigation of the interface formed by depositing Ag onto Si(111) under various conditions. A wealth of information exists in the literature covering various aspects of this system, especially for the surface reconstructions at low coverages. This abundance of information is partially due to Ag/Si(111) being a "prototypical nonreactive" system; Ag and Si are chemically nonreactive and do not intermix up to several hundred degrees Celsius. For this very reason, it is expected to exhibit relatively simple behaviors. We investigated three distinct sample configurations. These were (1) a "thick" Ag film with a thickness of a few hundred angstroms deposited on a Si(111)-(7×7) surface maintained at room temperature (RT), (2) the same as (1) except for a post-deposition anneal at 400°C, and (3) a Ag monolayer deposited on Si(111) annealed to form the ( $\sqrt{3}\times\sqrt{3}$ )R30° surface reconstruction,<sup>13-18</sup> further covered by a thick Ag film prepared by deposition at room temperature. These interfaces will be referred to as Ag/Si(7×7), Ag/Si(1×1), and Ag/Si( $\sqrt{3}\times\sqrt{3}$ ):Ag, respectively. The (7×7) and (1×1) notations for the first two sample configurations will become clear as our in-plane x-ray scans show the interface symmetry to be (7×7) and (1×1), respectively. In other words, the post-deposition anneal converts the (7×7) interface reconstruction to (1×1). For the last sample, the ( $\sqrt{3}\times\sqrt{3}$ ) designation refers to the beginning surface reconstruction before the deposition of a thick Ag film at RT; after the deposition, this ( $\sqrt{3}\times\sqrt{3}$ ) reconstruction is lifted, and the resulting interface is (1×1). For simplicity, this (1×1) symmetry is not included in the notation.

## II. EXPERIMENTAL DETAILS

The samples were prepared in two ultrahigh vacuum (UHV) molecular-beam epitaxy (MBE) chambers at the University of Illinois. The Si(111) substrates were cut from commercially available *n*-type wafers with 1–30- $\Omega$  cm resistivities. The samples were outgassed at 400°C and cleaned by resistive heating to 1100°C for 7–15 s. This method consistently produces well-ordered (7×7) surfaces as verified by reflection high-energy electron diffraction (RHEED). The samples were allowed to cool to RT before Ag film growth. Ag of 99.9999% purity was evaporated from either a feedback controlled electron-beam heated Mo crucible or an effusion cell, and the deposition was monitored by a water-cooled quartz thickness monitor with measured rates between 1.0 to 3.3 Å/min. The Ag/Si(7×7) samples were fabricated by depositing a "thick" Ag film (thicknesses of 250–650 Å) on the room-temperature Si(111)-(7×7) substrate. The Ag/Si(1×1) samples were fabricated in the same way, except for the extra step of a post-deposition anneal at 400°C for one minute. The Si( $\sqrt{3}\times\sqrt{3}$ ):Ag substrates were formed by depositing one ML of Ag onto a RT Si(111)-(7×7) surface followed by a one-minute anneal at 400°C. After the ( $\sqrt{3}\times\sqrt{3}$ )R30° surface reconstruction was confirmed by RHEED and after the sample had cooled down to RT, a thick Ag film was deposited upon it to form the Ag/Si( $\sqrt{3}\times\sqrt{3}$ ):Ag samples.

All of the x-ray measurements involving diffraction from the interface were carried out at the National Synchrotron Light Source, Brookhaven National Laboratory, on beamline X-14A. X-ray wavelengths of 1.1167 and 1.5916 Å were used. The samples were enclosed within an evacuated Be dome to reduce air scattering. A few of the Ag film thicknesses determined from the rate measurements using the quartz thickness monitor were checked by x-ray reflectivity measurements of the film interference patterns; the results agree within experimental uncertainty. For some of the less demanding diffraction measurements characterizing the Ag film itself, the experiment was carried out using an in-house rotating anode source, since diffraction from the film is much more intense than diffraction from the interface.

## III. RESULTS AND DISCUSSION

### A. Reflection high-energy electron-diffraction (RHEED) observations

Preliminary characterization of the Ag film was performed using the RHEED systems available in both MBE chambers. The *in situ* RHEED observations during growth of the Ag film on the Si(111)-(7×7) substrate at RT showed a Ag(111)-(1×1) diffraction pattern in parallel epitaxy with some twinning for Ag coverages beyond 1 ML and up to a final thickness of several hundred angstroms. Post deposition RHEED showed a reasonably good quality Ag(111)-(1×1) pattern; the streaks were somewhat fuzzy. The growth can be described as approximately layer by layer. After a 1-min 400°C anneal of the RT prepared film, the RHEED pattern improved and became a sharp Ag(111)-(1×1). The

lattice constant of the Ag film both before and after the anneal is identical to that of bulk Ag within experimental resolution. The films appeared mirrorlike by visual inspection for both the unannealed Ag/Si(7×7) sample and the annealed Ag/Si(1×1) sample.

RHEED observations following an identical anneal after deposition of only one ML of Ag on Si(111)-(7×7) exhibited the  $(\sqrt{3} \times \sqrt{3})R30^\circ$  pattern. After RT deposition of hundreds of angstroms of Ag onto this Si(111)- $(\sqrt{3} \times \sqrt{3})$ :Ag surface, RHEED showed a very fuzzy Ag(111)-(1×1) pattern, similarly oriented as described above, accompanied by a few diffuse polycrystalline powder rings. The background was high. In contrast to the uniform mirrorlike finish seen from the Ag/Si(7×7) and Ag/Si(1×1) samples described above, the Ag/Si( $\sqrt{3} \times \sqrt{3}$ ):Ag samples had faint milky or foggy splotches on top of the silvery finish. Our observations are supported by a number of other studies on this system.<sup>4,19-24</sup>

### B. Difference in growth mode

Based on the above RHEED and visual observations, the RT growth of Ag on Si( $\sqrt{3} \times \sqrt{3}$ ):Ag appears to be three dimensional, while the corresponding growth on Si(111)-(7×7) is nearly layer by layer. One parameter governing the growth mode is the substrate surface free energy, and three-dimensional growth is favored when the substrate surface free energy is low. Since the Si(111)-( $\sqrt{3} \times \sqrt{3}$ ):Ag surface is obtained by thermal annealing, it must have a lower surface energy than the corresponding unannealed system. This could provide an explanation for the observed difference in growth mode.

### C. Interface symmetry and structure of Ag/Si(111)-(7×7) as observed by diffraction

A hexagonal  $(hkl)_{\text{hex}}$  surface coordinate system is used here to describe the x-ray-diffraction results. Details of this coordinate system for the Si(111) surface have been discussed elsewhere.<sup>25</sup> Figure 1 is a schematic vertical cross-section drawing along a high-symmetry direction in reciprocal space for the Ag/Si(111) system. The momentum transfer is denoted by  $(hkl)_{\text{hex}}$ . The cubic  $(hkl)$  Miller indices of bulk Ag and Si Bragg points are indicated, and symmetry-forbidden Si Bragg points are marked by a crossed circle. The Bragg points lie along crystal truncation rods indicated in the figure by vertical lines. Note that the Ag and Si rods are at different locations due to their different lattice constants, and there is generally no interference from the Ag(111) overlayer structure when the Si features are scanned.

To determine the symmetry of the interface reconstruction, we employed in-plane  $\omega$ -rocking curve scans as well as in-plane ( $l \approx 0$ ) scans along linear segments in reciprocal space, which we will refer to as “ $k$  scans.” As mentioned earlier, the interface formed by depositing Ag on RT Si(111)-(7×7) shows a (7×7) symmetry. Figure 2 is a portion of a  $k$  scan along the  $[01]_{\text{hex}}$  direction through the Si(01)<sub>hex</sub> rod. In addition to the intense (01)<sub>hex</sub> rod, the  $(0\frac{6}{7})_{\text{hex}}$  superstructure peak is clearly

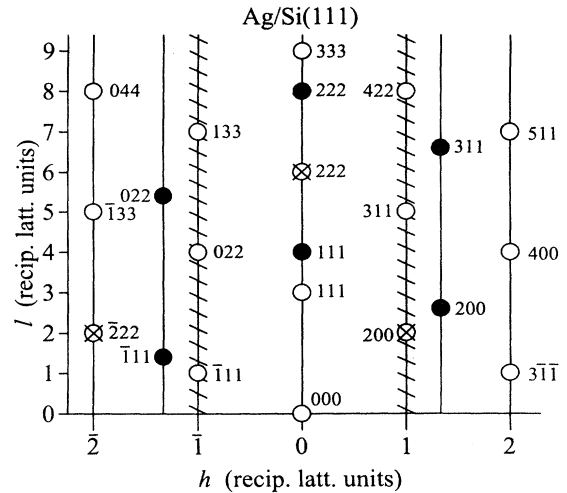


FIG. 1. Schematic vertical cross-section drawing of reciprocal space for the Ag/Si(111) system along the  $[2\bar{1}\bar{1}]$  high-symmetry direction. The surface  $(hkl)_{\text{hex}}$  hexagonal coordinate system is shown along with the cubic  $(hkl)$  Miller indices of both the bulk Si Bragg points (open circles) and Ag Bragg points (filled circles). Crossed open circles represent symmetry forbidden Si Bragg points. Truncation rods are indicated by vertical lines. The hatched truncation rods are the ones scanned in our experiment.

visible, and its intensity relative to the  $(01)_{\text{hex}}$  rod is comparable in order of magnitude to what has been reported in the literature for clean Si(111)-(7×7) in vacuum. As additional examples, Figs. 3(a) and 3(b) show in-plane  $\omega$ -rocking curves at the  $(\frac{6}{7}0)_{\text{hex}}$  and  $(\frac{8}{7}0)_{\text{hex}}$  seventh-order rod positions, respectively. Similar rocking curves were taken at other seventh-order rod positions, and many were found to have significant diffraction intensities. Survey scans through many line segments in reciprocal space reveal that the interface symmetry is

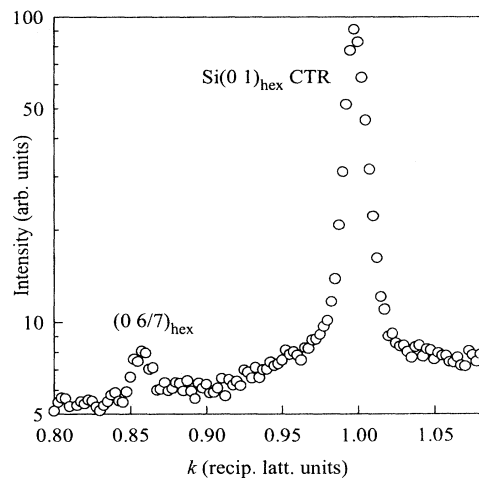


FIG. 2. In-plane reciprocal space line scan around the Si(01)<sub>hex</sub> truncation rod of the Ag/Si(7×7) interface. The scan is along the  $(0k)_{\text{hex}}$  high-symmetry direction. The  $(0\frac{6}{7})_{\text{hex}}$  superstructure peak is indicated.

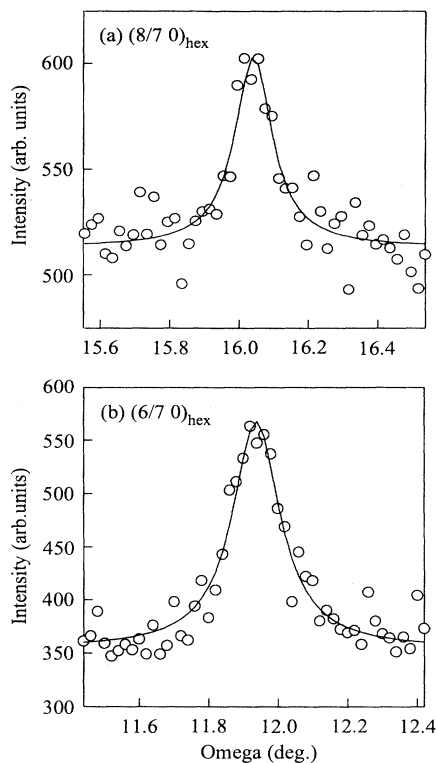


FIG. 3. In-plane  $\omega$ -rocking curves of the seventh-order peak positions (a)  $(\frac{8}{7} 0)_{\text{hex}}$  and (b)  $(\frac{6}{7} 0)_{\text{hex}}$  for the Ag/Si(7 $\times$ 7) interface. The solid line is a Lorentzian fit to the data.

(7 $\times$ 7), with no mixtures of other symmetries including  $(\sqrt{3}\times\sqrt{3})R30^\circ$ .

The preservation of the (7 $\times$ 7) symmetry at the interface is a consequence of the weak interaction between Ag and Si, which did not intermix or form compounds. The relative intensity distributions of the seventh-order fractional peaks from our measurements are somewhat similar to those obtained in UHV from a clean Si(111)-(7 $\times$ 7) surface,<sup>26,27</sup> but there are quantitative differences, indicating a difference in structure. In similar Si(111) interface studies, Gibson *et al.*<sup>7</sup> and Akimoto *et al.*<sup>9</sup> studying Si(111)-(7 $\times$ 7) capped by amorphous Si both noted intensity differences in their measurements of seventh-order peaks from the UHV clean Si surface. These differences have been attributed to the destruction of the adatom periodic structure. The (7 $\times$ 7) reconstruction of the Si(111) surface is known to consist of a surface stacking fault in one half of the (7 $\times$ 7) unit cell, and both the normal and reverse stacked halves of the unit cell are decorated by adatoms. These adatoms are weakly bonded, and are thus likely to be disturbed by Ag deposition in our case. However, Tosch and Neddermeyer conducted a scanning-tunneling-microscopy experiment investigating the initial stages of Ag growth on Si(111)-(7 $\times$ 7) at Si substrate temperatures of 90°C and 130°C.<sup>21</sup> They observed the Ag islands reflected details of the (7 $\times$ 7) reconstruction, and in some cases saw the underlying adatom structure reflected in the Ag islands. This led them to interpret that the (7 $\times$ 7) structure was largely preserved under the Ag islands. A direct comparison is

not possible, strictly speaking, since we prepared our sample at RT and for a much thicker film. A reordering of the interface was actually observed in our experiment when the sample temperature was raised (see below). We believe that our intensity differences for RT prepared samples result from the removal of the periodicity of the adatom network during deposition, in agreement with the observations made by Gibson and Akimoto. In other words, the Si adatom positions are likely perturbed out of registry relative to the substrate lattice by the Ag deposition. The atomic movement does not have to be very far before the effective Debye-Waller-like factor eliminates the adatom contribution to the diffraction intensity. The retention of the (7 $\times$ 7) periodicity is mainly due to the durability of the stacking fault. To reverse the stacking fault, a large number of atoms and bonds would have to be rearranged.

To deduce information about the stacking of atomic layers at the interface, we scanned the Si(1 0)<sub>hex</sub> truncation rod, with  $l$  spanning both positive and negative values. The hatched lines in Fig. 1 highlight the two segments of the Si(1 0)<sub>hex</sub> crystal truncation rod; the  $(\bar{1} 0 l)_{\text{hex}}$  rod with  $l$  positive is symmetry equivalent to  $(1 0 \bar{l})_{\text{hex}}$ . In our diffraction geometry where the incident and diffracted beams are both on the same side of the surface, physical access to negative  $l$  values is denied. Figure 4(a) shows the integrated intensity rod profile. Sub-

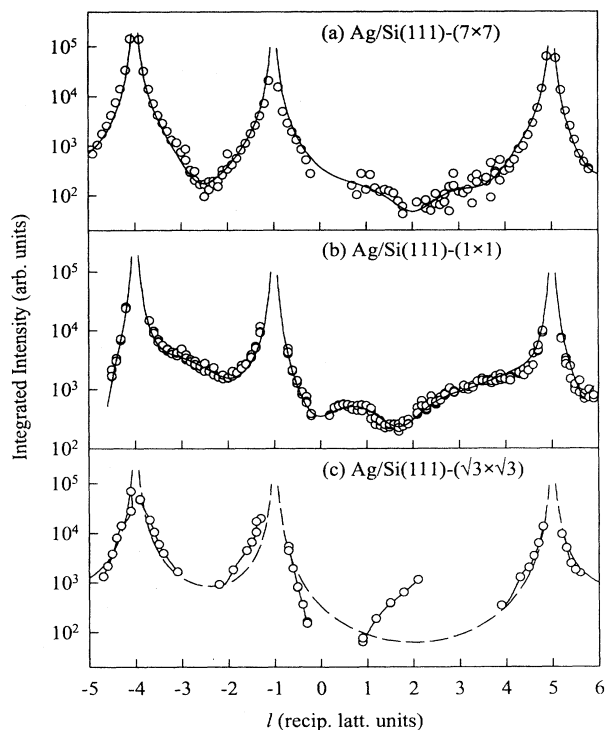


FIG. 4. The Si(1 0  $l$ )<sub>hex</sub> truncation rods for (a) Ag/Si(7 $\times$ 7), (b) Ag/Si(1 $\times$ 1), and (c) Ag/Si( $\sqrt{3}\times\sqrt{3}$ ):Ag, respectively. The circles are data points. The curves in (a) and (b) are best fits. The solid curve in (c) simply connects the data points, while the dashed curve indicates the theoretical double-layer bulk-terminated Si(111) surface for comparison.

strate Bragg peaks are located at  $l = -4, -1, \text{ and } 5$  (the  $l = 2$  peak is symmetry forbidden). The data points are shown by circles. Multiple scans were taken at various  $l$  values and their spread is an experimental indication of the error associated with the measurement.

Since our in-plane diffraction measurements suggest a  $(7 \times 7)$  structure with the adatoms out of registry, our model for the Si at the interface is shown in Fig. 5. The Si lattice in the bulk consists of double layers arranged in the fcc stacking sequence. The top layer, however, consists of an equal combination of normal stacking and reverse stacking. To fit the truncation rod profile, we allow the top four atomic layers, as labeled in the figure, to relax relative to the bulk in the direction normal to the surface. We also allow the atomic occupancy for each of the two top layers to differ from unity. This fractional occupancy simulates the effect of random disturbance on atomic positions caused by the Ag deposition (Debye-Waller-like attenuation). There are only six free parameters for the structure in the model, four for layer relaxations  $\Delta z_i$ , with  $i = 1-4$ , and two for fractional occupancies  $a_3$  and  $a_4$ . The result of our fit of the rod profile, shown as a curve in Fig. 4(a), agrees with the data well. Numerous fits were tried; using additional free parameters such as  $a_1$  and  $a_2$  did not yield any significantly better results. The final values of the parameters are  $\Delta z_{1-4} = 0.054, 0.016, -0.092, \text{ and } 0.47 \text{ \AA}$ , respectively, and  $a_3 = 0.38$  and  $a_4 = 0.35$ .<sup>28</sup> These  $\Delta z$  values are very small, except for the top layer, which is in direct contact with the Ag. The two fractional occupancies are less than unity as expected, implying that many of the Si atoms in these layers are displaced from their ideal positions and are no longer scattering coherently along the rod. The austerity of the model, the reasonable resulting values for the layer occupancies and relaxations, and the good fit demonstrate that the model contains the correct gross interfacial features.

#### D. Thermally induced transformation to Ag/Si(111)-(1 × 1)

We investigated the structural phase transformation of the  $(7 \times 7)$  interface caused by annealing. One might expect intuitively the well documented and stable Si(111)-

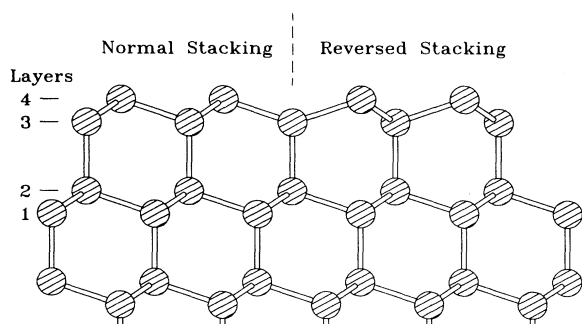


FIG. 5. Side view of a structural model for the Si(111) substrate under the Ag overlayer. The top four layers are labeled 1-4.

$(\sqrt{3} \times \sqrt{3})$ :Ag structure, observed for monolayer Ag coverage at high temperatures, to form at the interface. However, this is not the case. We monitored the most intense seventh-order and  $(\sqrt{3} \times \sqrt{3})R 30^\circ$  superstructure peak positions as we annealed the sample. Figure 6 is a graph of the evolution of the  $(\frac{6}{7} 0)_{\text{hex}}$  peak intensity as a function of annealing temperature; each data point corresponds to an anneal at the indicated temperature for 5 min. Around  $150^\circ\text{C}$ , the intensity modestly increases indicating thermodynamic ordering; in other words, the part of the  $(7 \times 7)$  reconstruction damaged by the Ag deposition becomes partially restored. Between  $200$ – $250^\circ\text{C}$ , the peak vanishes and the intensity drops to zero. This transition temperature is close to the  $(\sqrt{3} \times \sqrt{3})$ :Ag formation temperature for the monolayer-covered surface, suggesting that this temperature is characteristic for substantial atomic movement. Scans of the most intense UHV Si( $\sqrt{3} \times \sqrt{3}$ ):Ag superstructure positions, including  $(\frac{4}{3} \frac{1}{3})_{\text{hex}}$ ,  $(\frac{2}{3} \frac{2}{3})_{\text{hex}}$ , and  $(\frac{5}{3} \frac{2}{3})_{\text{hex}}$ , showed no evidence of any interface peaks before or after annealing. Additional in-plane  $k$  scans along high-symmetry lines for the annealed sample revealed no periodic superstructure peaks. Figure 7(a) is one such scan along the  $[1 0]_{\text{hex}}$  direction. Thus, the interface structure is  $(1 \times 1)$  after the anneal.

This  $(1 \times 1)$  structure at the interface is perhaps not surprising. The driving force for surface reconstruction is dominated by two competing factors: one is to minimize the number of surface dangling bonds, and the other is to minimize the surface strain caused by atomic rearrangement. Ag is a free-electron-like metal, and can be modeled quite well by a jellium. The delocalized conduction electrons in the Ag film can provide a good termination for any arrangements of the dangling bonds on the Si substrate. Thus, the number and position of dangling bonds are apparently not an issue here. It is, therefore, reasonable to expect, based on bond strain considerations, that the structure of the Si substrate after annealing should be a bulk-like  $(1 \times 1)$ .

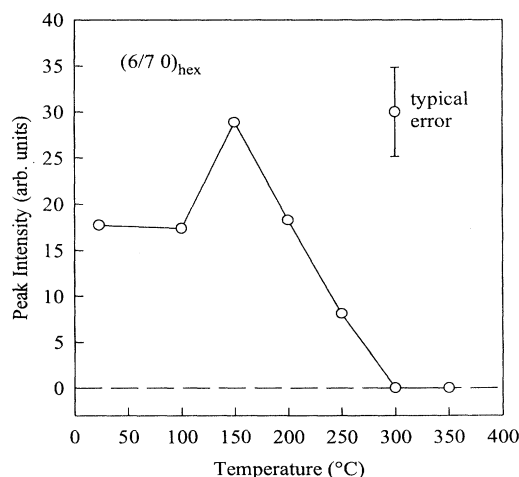


FIG. 6. Evolution of the intensity of the  $(\frac{6}{7} 0)_{\text{hex}}$  peak for Ag/Si( $7 \times 7$ ) as a function of annealing temperature.

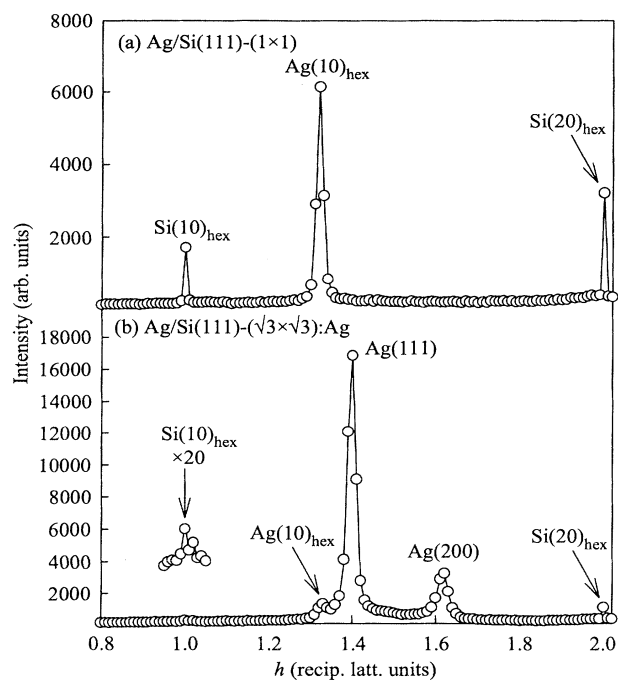


FIG. 7. In-plane reciprocal space line scan along the  $(h\ 0)_{\text{hex}}$  high-symmetry direction for (a) the annealed Ag/Si(1 $\times$ 1) and (b) the Ag/Si( $\sqrt{3}\times\sqrt{3}$ ):Ag interface. Si substrate and Ag over-layer rods are indicated by  $(hk)_{\text{hex}}$  indices, while powder rings are denoted by cubic  $(hkl)$  Miller indices.

#### E. Interface structure of Ag/Si(111)-(1 $\times$ 1) as observed by diffraction

To verify the above idea about the interface structure, the Si(1 0  $l$ )<sub>hex</sub> truncation rod was measured. The results are shown in Fig. 4(b). Clearly, there are significant differences in the rod profile induced by the annealing. For example, the overall intensity in the “valley” between the Bragg peaks at  $l = -1$  and 5 becomes substantially higher. This intensity is a measure of the amount of scattering from the interface. To fit the data, our model is a simple bulk-terminated Si(111)-(1 $\times$ 1) surface with fractional layer occupancies and layer relaxations (see Fig. 5; ignore the reversed stacking part). The result of the fit is shown as the curve in Fig. 4(b), which describes the data well. The final values of the parameters are  $\Delta z_{1-4} = -0.077, -0.10, -0.02,$  and  $0.19\ \text{\AA}$ , respectively, and  $a_2 = 0.85, a_3 = 0.96,$  and  $a_4 = 1.33$ .<sup>28</sup> Again, the layer relaxations are very small and reasonable. Note, however, that  $a_4$  is greater than unity. This follows naturally from the fit, due to the increased scattering from the interface. The high intensity in the valley between the  $l = -1$  and 5 Bragg peaks, as noted above, can be accounted for only if extra scattering is associated with the interface. One simple explanation for  $a_4$  being greater than unity is that the top layer in our model is in fact an alloy consisting of some Ag in a mostly Si layer. Since Ag has a much larger scattering factor than Si (47 vs 14), a small Ag admixture will boost the effective fractional occupancy to a value much greater than unity. This in-

terpretation is consistent with a commonly observed phenomenon; that is, even though two materials are immiscible in the bulk, they can form monolayer alloys at a boundary. For example, such monolayer mixing has been reported by Pleth Nielsen *et al.* in the case of Au/Ni(110).<sup>29</sup> This phenomenon has also been explained by theory.<sup>30</sup>

The annealed Ag/Si(111)-(1 $\times$ 1) interface has previously been studied by LeGoues *et al.*<sup>31</sup> using plan-view and cross-section transmission electron microscopy (TEM). They examined samples both grown at elevated temperatures and those annealed after RT deposition. Their TEM images show an abrupt boundary between these two materials, which is consistent with the mutual insolubility of these two materials in the bulk. Further, the Ag lattice constant appears to be the same as the bulk Ag value, in agreement with our finding. Based on an old, and probably incorrect model of the Si( $\sqrt{3}\times\sqrt{3}$ ):Ag surface structure (see below), they proposed a model consisting of a Ag layer incorporated into the Si lattice and located beneath the topmost Si layer. Our data do not support their model. Figure 8 displays the theoretical truncation rod profile for this buried Ag layer interface model, which is compared with our fit based on the surface alloy model and the predicted profile for an ideal Si-double-layer-terminated surface. The buried Ag layer model contains a full Ag layer located at subsurface  $H_3$  sites of the Si(111) substrate. This is our best estimation of the model of LeGoues, Leibr, and Reiner,<sup>31</sup> since atomic positions of this Ag layer were not completely specified in their paper. A large discrepancy is seen, and the overall scattering intensity in the valley region is clearly much too high. This high intensity is caused by the very strong scattering of the Ag relative to Si. A reduced layer occupancy reduces the discrepancy. We have tried many other related models in the fit, including partial Ag layers registered in the  $T_4$ , on-top, and replacement sites. The replacement model is just our surface alloy model, and it is the only model that provides a good fit to the data, reproducing the bumps and dips in the intensity profile at the right locations.

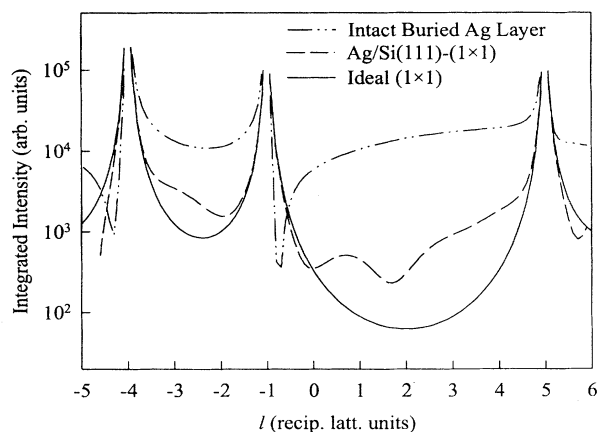


FIG. 8. Comparison of Si(1 0  $l$ )<sub>hex</sub> truncation rods for a buried Ag layer model, a Si-double-layer-terminated surface, and our surface alloy model fit for the annealed Ag/Si(1 $\times$ 1).

### F. Interface symmetry and structure of Ag/Si( $\sqrt{3}\times\sqrt{3}$ ):Ag

With no evidence for the ( $\sqrt{3}\times\sqrt{3}$ )R30° reconstruction at the annealed interface, we capped a Si( $\sqrt{3}\times\sqrt{3}$ ):Ag ML surface with a Ag film. These samples also showed no evidence of the ( $\sqrt{3}\times\sqrt{3}$ )R30° structure at the interface, as demonstrated by careful rocking curve scans at many ( $\sqrt{3}\times\sqrt{3}$ )R30° locations. The symmetry of the interface is (1×1). As mentioned earlier, the Ag film was visibly rough and exhibited a number of powder rings in the diffraction pattern. An example of a  $k$  scan is shown in Fig. 7(b), where the Ag(111) and Si(111) rod positions are indicated. The features, not seen in Fig. 7(a) and incommensurate relative to the Si peak positions, can be explained by the Ag powder rings. These rings, with an intense broad tail, also intercept the Si(1 0  $l$ )<sub>hex</sub> truncation rod, rendering a significant portion of the rod immeasurable. The parts that we can measure are shown in Fig. 4(c), which are not enough for a detailed structural modeling.

Even though we cannot model the structure, it is obvious from the data that this interface is different from the other two interfaces. The atomic structure of the ML-covered Si( $\sqrt{3}\times\sqrt{3}$ ):Ag surface has been a subject of considerable debate, and it now appears to be generally accepted to consist of a honeycomb-chained-trimer layer of Ag on top of a Si lattice terminated halfway between a double layer.<sup>13–18</sup> The fact that Ag and Si do not form bulk chemical compounds imply that these Ag-Si bonds at the surface must be rather weak. Thus, it is perhaps not surprising that the trimer array of Ag surface atoms could become perturbed with further Ag deposition to lose their ( $\sqrt{3}\times\sqrt{3}$ )R30° registry relative to the substrate, as observed in our experiment. This loss of adatom registry is similar to the Ag/Si(7×7) case. For Ag/Si(7×7), the structurally robust stacking fault feature remains to keep the (7×7) symmetry, but there is no such corresponding structural feature for the Si( $\sqrt{3}\times\sqrt{3}$ ):Ag interface.

The lack of a ( $\sqrt{3}\times\sqrt{3}$ ):Ag structure at the boundary in either the annealed or covered case is evidence that this structure is only a surface effect. In this particular case, the interface structure is unrelated to the adsorbate ML structure.

### G. Property-structure relationship

The different atomic structure at the interface is likely to give rise to different interface properties. As mentioned in the Introduction, one of the goals of interface studies is to establish the relationship between structure and properties. For the two well-characterized interfaces, Ag/Si(7×7) and Ag/Si(1×1), the main qualitative structural difference between them is the presence of a stacking fault in the former, but not in the latter. In comparing the electrical performance of these two interfaces, Schmitsdorf *et al.* found the Schottky barrier for the Ag/Si(1×1) system to be 0.78 eV; this is 0.07 eV greater than the Ag/Si(7×7) interface.<sup>5</sup> It is likely that the stacking fault is associated with an electric dipole layer relative to the unfaulted structure, leading to this difference in Schottky barrier height.

### H. Structure of the Ag overlayer

Our RHEED observations of the Ag overlayer film provided only a qualitative indication of the film quality and epitaxial relationship. More detailed information is available from x-ray-diffraction measurements. In-plane  $k$  scans of both the Ag/Si(7×7) and Ag/Si(1×1) interfaces clearly show the Ag overlayer film to be incommensurate. The Ag and Si lattice constants have a ratio of approximately 3:4. The mismatch is only about 0.3% between the larger cells of (3×3) Si and (4×4) Ag. Nevertheless, the Si(4 0)<sub>hex</sub> and Ag(3 0)<sub>hex</sub> rods do not coincide for the Ag/Si(1×1) interface, indicating that the two lattices remain incommensurate up to this dimension.

Figure 9(a) is a scan measuring the diffraction along the specular direction to determine the texture of the Ag film on the Ag/Si(1×1) sample. It shows the overlayer film to be a predominantly well-ordered Ag(111) film. Much longer and higher intensity scans (lower panel) exhibit evidence of {200} and {311} oriented grains in the film, which combined to make up less than 0.1% of the film volume. Whereas similar scans of the Ag/Si( $\sqrt{3}\times\sqrt{3}$ ):Ag sample show the Ag film to have fewer well-ordered Ag(111) crystallites and more {200} and {311} grains amounting to nearly 13% of the film volume as seen in the two panels of Fig. 9(b). This latter capping film also has a powder component seen by both RHEED and x-ray diffraction, and the surface has a milky visual appearance indicating graininess.

For the Ag/Si(111)-(1×1) samples,  $\phi$  scans were taken of the Ag{111} Bragg peaks to determine the orientational epitaxy of the film. These scans show the expected threefold symmetry. Figure 10 shows  $\phi$  scans of the Si{111}, Ag{111}, and Ag{220} Bragg peaks for this sample. A number of previous studies of Ag film growth on Si(111) have found RT prepared films and annealed

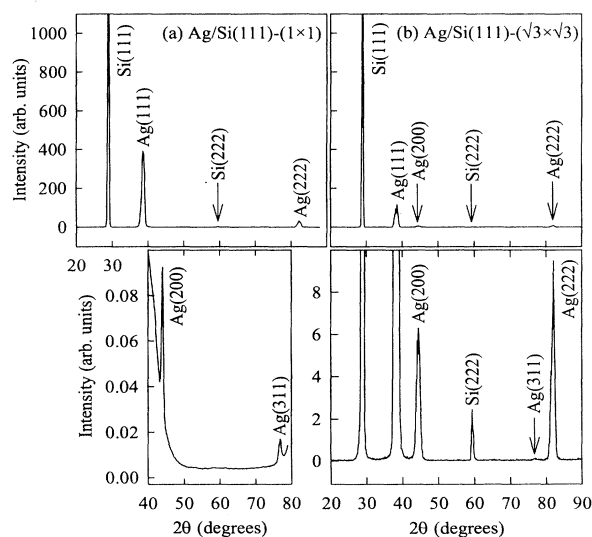


FIG. 9. Scans measuring diffraction along the specular direction of (a) the annealed Ag/Si(1×1) and (b) the Ag capped Ag/Si( $\sqrt{3}\times\sqrt{3}$ ):Ag. For each sample, the lower panel shows the result of a longer scan to reveal weaker features.

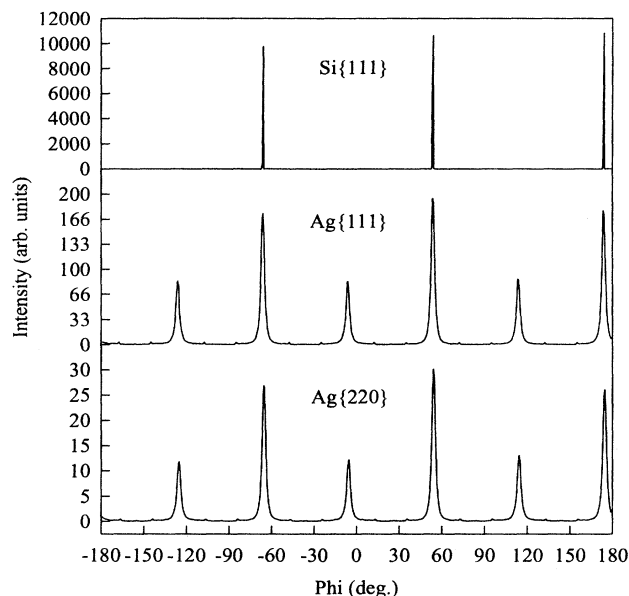


FIG. 10.  $\phi$  scans of Si and Ag Bragg peaks for the annealed Ag/Si(1 $\times$ 1) illustrating the Ag overlayer film twinned epitaxial relationship to the Si(111) substrate.

films after RT growth exhibit twin structures.<sup>31–33</sup> These twins both exhibit the (111) orientation, and are conventionally called type-*A* and -*B* epitaxy; type *A* has Ag[110] parallel to Si[110], while type *B* is rotated by 180° about the surface normal. From our  $\phi$  scans shown in Fig. 10, we measured an *A*:*B* ratio of 2:1 for our annealed film.

#### IV. CONCLUSIONS

These structural interface experiments on the three characteristic Ag/Si(111) interfaces have yielded a number of noteworthy results. The Si(111)-(7 $\times$ 7) periodicity is preserved under a RT deposited thick Ag film. Even though the adatoms are displaced, the (7 $\times$ 7) stacking fault persists at this Ag-modified (7 $\times$ 7) interface. This interface reconstruction is metastable. Annealing this interface above 200–250°C, which is close to the ( $\sqrt{3}\times\sqrt{3}$ ):Ag formation temperature for the monolayer-Ag covered Si(111) surface, does not convert the (7 $\times$ 7) interface to this ( $\sqrt{3}\times\sqrt{3}$ )R30° structure; rather the interface structure transforms from (7 $\times$ 7) to (1 $\times$ 1). The (7 $\times$ 7) stacking fault is removed after the transition, and a small amount of Ag becomes alloyed into the top Si layer. The Ag film remains a predominantly well-ordered Ag(111) film with both *A*- and *B*-type epitaxial orientations with an *A*:*B* ratio of 2:1. In

addition, in-plane *k* scans show that the Ag overlayer film is incommensurate with respect to the Si(111) substrate.

A RT Ag-capped Si( $\sqrt{3}\times\sqrt{3}$ ):Ag ML structure also showed no evidence whatsoever of any ( $\sqrt{3}\times\sqrt{3}$ ) periodicity. The periodicity of the interface became (1 $\times$ 1) after the deposition. RHEED and x-ray diffraction of these samples show the Ag capping film to have Ag(111), Ag(200), and Ag(311) oriented grains. A powder component is evident in the diffraction patterns, and the film is grainy. This demonstrates the ( $\sqrt{3}\times\sqrt{3}$ ):Ag structure is a poor template for single crystalline RT Ag film growth, and the reason is likely a reduced surface free energy induced by the annealing necessary for the formation of the ( $\sqrt{3}\times\sqrt{3}$ ):Ag surface structure.

Finally, we note that clean to ML-coverage surface structures are not necessarily related to the true interfacial structure. In the case of RT Ag film growth, the clean Si(111)-(7 $\times$ 7) surface is closely related to the resulting interface structure. However, the well-documented Si( $\sqrt{3}\times\sqrt{3}$ ):Ag ML structure usually observed after annealing above about 200°C is not seen at a buried interface after annealing. In addition, even a RT Ag-capped Si( $\sqrt{3}\times\sqrt{3}$ ):Ag ML structure shows no evidence of this ( $\sqrt{3}\times\sqrt{3}$ )R30° reconstruction exemplifying the necessity for case-by-case consideration to be given when relating surface structural characteristics to interfacial ones.

#### ACKNOWLEDGMENTS

This material is based upon work supported by the Division of Materials Sciences, Office of Basic Energy Sciences, U.S. Department of Energy, under Grant No. DEFG02-91ER45439 (University of Illinois). An acknowledgement is also made to the Illinois Board of Higher Education under Contract No. HECA-NWU-0950-9510A, to the Petroleum Research Fund, administered by the American Chemical Society, and to the National Science Foundation under Grant No. DMR-9223546 for partial equipment and/or personnel support. The National Synchrotron Light Source is supported by the U.S. Department of Energy under Contract No. DEAC02-76CH0016. Beamline X-14A is jointly operated by the Oak Ridge National Laboratory, Martin Marietta Energy Systems Inc. (supported by the Division of Materials Sciences and Division of Chemical Sciences, Office of Basic Energy Sciences, U.S. Department of Energy under Contract No. DEAC05-84OR21400), and by the University of Illinois Frederick Seitz Materials Research Laboratory.

<sup>1</sup>For a recent review of metal-semiconductor interfaces, see L. J. Brillson, *Surf. Sci.* **299/300**, 909 (1994).

<sup>2</sup>R. T. Tung, *Phys. Rev. Lett.* **52**, 461 (1984).

<sup>3</sup>D. R. Heslinga, H. H. Weitering, D. P. van der Werf, T. M. Klapwijk, and T. Hibma, *Phys. Rev. Lett.* **64**, 1589 (1990).

<sup>4</sup>H. H. Weitering, J. P. Sullivan, R. J. Carolissen, W. R. Gra-

ham, and R. T. Tung, *Appl. Surf. Sci.* **70/71**, 422 (1993).

<sup>5</sup>R. F. Schmitsdorf, T. U. Kampen, and W. Mönch, in *Proceedings of the First International Conference on Control of Semiconductor Interfaces*, Karuizawa, Japan, 1993, edited by I. Ohdomari, M. Oshima, and A. Hiraki (Elsevier, New York, 1994).

- <sup>6</sup>W. Mönch, Surf. Sci. **299/300**, 928 (1994).
- <sup>7</sup>J. M. Gibson, H.-J. Gossmann, J. C. Bean, R. T. Tung, and L. C. Feldman, Phys. Rev. Lett. **56**, 355 (1986).
- <sup>8</sup>D. Loretto, J. M. Gibson, and S. M. Yalisove, Phys. Rev. Lett. **63**, 298 (1989).
- <sup>9</sup>K. Akimoto, J. Mizuki, I. Hirose, and J. Matsui, Appl. Surf. Sci. **41/42**, 317 (1989).
- <sup>10</sup>Hawoong Hong, R. D. Aburano, D.-S. Lin, H. Chen, T.-C. Chiang, P. Zschack, and E. D. Specht, Phys. Rev. Lett. **68**, 507 (1992).
- <sup>11</sup>Hawoong Hong, W. E. McMahon, P. Zschack, D.-S. Lin, R. D. Aburano, H. Chen, and T.-C. Chiang, Appl. Phys. Lett. **61**, 3127 (1992).
- <sup>12</sup>Hawoong Hong, R. D. Aburano, E. S. Hirschorn, P. Zschack, H. Chen, and T.-C. Chiang, Phys. Rev. B **47**, 6450 (1993).
- <sup>13</sup>T. Takahashi, S. Nakatani, N. Okamoto, T. Ishikawa, and S. Kikuta, Jpn. J. Appl. Phys. **27**, L753 (1988).
- <sup>14</sup>E. Vlieg, A. W. Denier van der Gon, J. F. van der Veen, J. E. MacDonald, and C. Norris, Surf. Sci. **209**, 100 (1989).
- <sup>15</sup>E. Vlieg, E. Fontes, and J. R. Patel, Phys. Rev. B **43**, 7185 (1991).
- <sup>16</sup>M. Katayama, R. S. Williams, M. Kato, E. Nomura, and M. Aono, Phys. Rev. Lett. **66**, 2762 (1991).
- <sup>17</sup>S. Watanabe, M. Aono, and M. Tsukada, Phys. Rev. B **44**, 8330 (1991).
- <sup>18</sup>Y. G. Ding, C. T. Chan, and K. M. Ho, Phys. Rev. Lett. **67**, 1454 (1991).
- <sup>19</sup>G. Le Lay, G. Quentel, J. P. Faurie, and A. Masson, Thin Solid Films **35**, 273 (1976).
- <sup>20</sup>G. Le Lay, G. Quentel, J. P. Faurie, and A. Masson, Thin Solid Films **35**, 289 (1976).
- <sup>21</sup>St. Tosch and H. Neddermeyer, Phys. Rev. Lett. **61**, 349 (1988).
- <sup>22</sup>S. Hasegawa and S. Ino, Surf. Sci. **283**, 438 (1993).
- <sup>23</sup>S. Hasegawa and S. Ino, Int. J. Mod. Phys. B **7**, 3817 (1993).
- <sup>24</sup>A. Endo and S. Ino, Surf. Sci. **293**, 165 (1993).
- <sup>25</sup>I. K. Robinson, W. K. Waskiewicz, R. T. Tung, and J. Bohr, Phys. Rev. Lett. **57**, 2714 (1986).
- <sup>26</sup>I. K. Robinson, W. K. Waskiewicz, P. H. Fuoss, J. B. Stark, and P. A. Bennett, Phys. Rev. B **33**, 7013 (1986).
- <sup>27</sup>I. K. Robinson, W. K. Waskiewicz, P. H. Fuoss, and L. J. Norton, Phys. Rev. B **37**, 4325 (1988).
- <sup>28</sup>R. D. Aburano, J. M. Roesler, Hawoong Hong, D.-S. Lin, T.-C. Chiang, and P. Zschack, Surf. Sci. Lett. (to be published).
- <sup>29</sup>L. Pleth Nielsen, F. Besenbacher, I. Stensgaard, E. Lægsgaard, C. Engdahl, P. Stoltze, K. W. Jacobsen, and J. K. Nørskov, Phys. Rev. Lett. **71**, 754 (1993).
- <sup>30</sup>J. Tersoff, Phys. Rev. Lett. **74**, 434 (1995).
- <sup>31</sup>F. K. LeGoues, M. Liehr, and M. Reiner, in *Initial Stages of Epitaxial Growth*, edited by R. Hull, J. M. Gibson, and D. A. Smith, Proceedings of the Materials Research Society, Anaheim, California, 1987 (Publishers Choice Book Mfg. Co., Mars, Pennsylvania, 1987), Vol. 94, p. 121; F. K. LeGoues, M. Liehr, M. Renier, and W. Krakow, Philos. Mag. B **57**, 179 (1988).
- <sup>32</sup>Y. Gotoh and S. Ino, Thin Solid Films **109**, 255 (1983).
- <sup>33</sup>T. C. Nason, L. You, G.-R. Yang, and T.-M. Lu, J. Appl. Phys. **69**, 773 (1991).